Article

Miniaturized Multi-Platform Free-Space Laser-Communication Terminals for Beyond-5G Networks and Space Applications

Alberto Carrasco-Casado [1,*] , Koichi Shiratama [1], Dimitar Kolev [1], Fumie Ono [1], Hiroyuki Tsuji [1] and Morio Toyoshima [2]

[1] Space Communication Systems Laboratory, National Institute of Information and Communications Technology (NICT), Tokyo 184-8795, Japan; shiratama@nict.go.jp (K.S.); dkolev@nict.go.jp (D.K.); fumie@nict.go.jp (F.O.); tsuji@nict.go.jp (H.T.)

[2] Wireless Networks Research Center, National Institute of Information and Communications Technology (NICT), Tokyo 184-8795, Japan; morio@nict.go.jp

* Correspondence: alberto@nict.go.jp

Abstract: Beyond-5G (B5G) technology plays a pivotal role in the next generation of communication infrastructure to support the future Society 5.0, a concept introduced in the 5th Basic Plan for Science and Technology by the Japanese Cabinet to define the long-term growth strategy for reconciling economic development with the resolution of social issues through the promotion of science and technologies. Free-space laser communication is a key element in boosting the data transmission capabilities required for B5G applications. The NICT will complete in 2024 the first fully functional prototypes of a series of miniaturized laser-communication terminals for multiple platforms. These terminals are designed to adapt to a wide range of requirements to address scenarios where laser communications can offer a competitive, enhanced solution compared to existing technologies. This paper provides an overview of these terminals' capabilities and the plans for their functional validation, as well as preliminary data from the first full-system tests. A number of innovations integrated into the terminals are introduced, such as the manufacture of the smallest miniaturized EDFA with integrated HPA and LNA and full space qualification to date, the first-ever integration of a beam-divergence control system in a practical communication terminal, the development of the most compact Tbit/s-class modem prototype documented in the literature, and the smallest gimbal design integrated in a lasercom terminal. Furthermore, this paper outlines the mid-term plans for demonstration in the most significant realistic scenarios, emphasizing the use of High-Altitude Platform Stations (HAPSs) and ultra-small satellites.

Keywords: free-space optical communications; satellite communications; space lasercom; miniaturized terminals; B5G; CubeSat; HAPS; society 5.0

1. Introduction

"Society 5.0" is a concept proposed by the Japanese Cabinet in the 5th Basic Plan for Science and Technology [1], which defines growth strategies for Japan. The concept of Society 5.0 envisions a future society to be realized by the 2030s, reconciling economic development with the resolution of social issues through the promotion of science and technologies, such as robotics, big data, the IoT (Internet of Things), AI (artificial intelligence), blockchain, telepresence and cyberspace, e-health, and unmanned mobility. Beyond 5G (B5G) and 6G are critical elements of the next generation of communication infrastructure to support the technologies essential for Society 5.0 [2]. Additional studies highlight the transformative potential of B5G and 6G networks in enhancing connectivity and enabling new technological advancements [3–7].

Free-space optical communication (FSOC) is already a mature technology with abundant demonstrations confirming its potential [8]. FSOC is positioned to play an essential

role in B5G and 6G networks by providing the low-latency and high-capacity data transmission needed to support the demanding applications mentioned above. FSOC can not only support applications currently handled by RF but also enable entirely new applications. In particular, quantum communications represent a use case that is especially compatible with the optical technologies required for lasercom, which serves as an excellent platform to support them [9,10]. This emerging field has garnered significant interest worldwide and holds the potential to innovate the communication industry [11,12]. By leveraging the advanced capabilities of FSOC, the integration of quantum communication technologies can be realized, paving the way for unprecedented advancements in secure data transmission. The integration of these technologies in B5G and 6G infrastructures will enhance connectivity and bandwidth, addressing the increasing demands of modern communication networks and enabling new possibilities for technological advancement and societal development.

The Japanese National Institute of Information and Communications Technology (NICT) is a pioneer of this technology, with three decades of recognized experience. This began in 1994 with the world's first space laser-communication mission using the GEO satellite ETS-VI [13], followed by the first LEO-to-ground demonstration with the LEO satellite OICETS in 2006 [14], the first FSOC terminal onboard a microsatellite with the LEO satellite SOCRATES in 2014 [15], and the first bidirectional feeder link with the GEO satellite ETS-IX, scheduled for launch in 2025 [16–18] (see Figure 1).
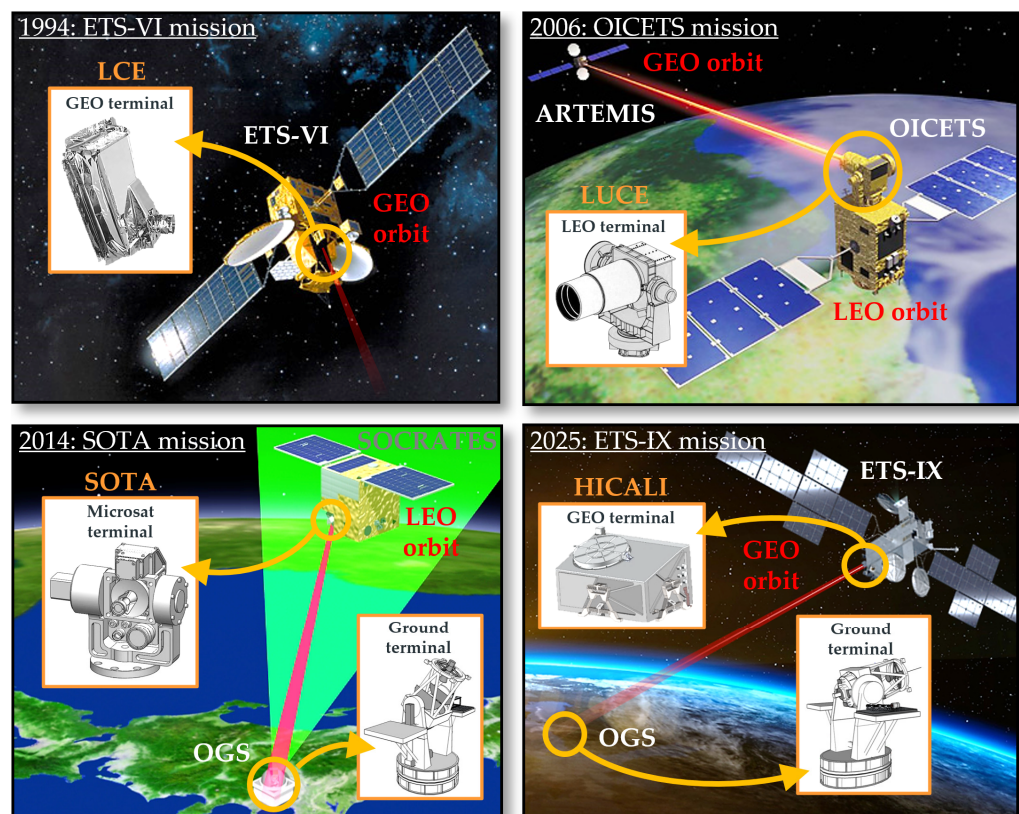

Figure 1. NICT's historical demonstration milestones.

All these past missions had a common necessity: evolving the technology from nearly zero to meet the specific requirements of each mission and repeating this process to address new challenges. However, once the basic technologies have been demonstrated and matured to become functional, this strategy is not optimum. Instead of the mission-oriented approach, a reutilization-oriented approach is pursued in the work described in this paper. The NICT identified the demand in the Japanese and global markets of a versatile terminal that can be reutilized across a variety of applications and initiated an endeavor to meet that need.

This manuscript introduces the NICT's ongoing efforts to develop a new series of miniaturized lasercom terminals, aiming to bridge the gap between demonstration and operational deployment in realistic scenarios. It provides an overview of their capabilities and the plans for their functional validation, as well as preliminary data from the first full-system tests. Additionally, this paper outlines mid-term plans for demonstrations in the most significant scenarios, emphasizing the use of High-Altitude Platform Stations (HAPSs) and ultra-small satellites.

Furthermore, this paper introduces and discusses several important innovations integrated into the terminals, such as the manufacture of the smallest miniaturized EDFA with integrated HPA and LNA and full space qualification to date, the first-ever integration of a beam-divergence control system in a practical communication terminal, the development of the most compact Tbit/s-class modem prototype documented in the literature, and the smallest gimbal design integrated in a lasercom terminal.

2. Practical FSOC Integration into B5G Networks

After several decades of research, free-space laser-communication technology has emerged as a pivotal element to fulfill the requirements of Non-Terrestrial Network (NTN) in the rapidly evolving landscape of B5G networks. The global B5G market's estimated value was close to USD 100 billion in 2022, and a projected growth rate in the magnitude of 50% annually is estimated from 2023 to 2030 [19,20]. 5G's faster speeds and low latency will enhance user experiences in applications like VR (Virtual Reality), AR (Augmented reality), gaming, seamless video calls, and high-definition videos. Taking into consideration the huge communication capabilities that will be required to support this increasingly demanding infrastructure, the potential impact of FSOC in the coming years cannot be overstated.

Although optical communications can potentially encompass a broad spectrum of applications, ranging from short-range links to deep space, there are a number of specific scenarios where free-space lasercom technologies will likely find their most compelling and realistic applications in the short and medium term, particularly within the context of B5G and 6G networks and space applications. These applications are shown in Figure 2 and can be described as follows:

1. Satellite constellations: In the context of Low Earth Orbit (LEO) satellite constellations, lasercom intersatellite links (ISLs) will play a vital role in amplifying network capacity. In the absence of atmospheric effects, these ISLs will enable seamless data transmission between satellites, boosting the efficiency and reach of the networks.
2. Direct from space to Earth: Optical downlinks from LEO satellites to the ground will enhance data retrieval from space. This application will have profound implications for various industries, including Earth observation and remote sensing, as well as a means to interconnect satellite constellations with ground networks.
3. HAPS repeaters: FSOC's reach will extend to High-Altitude Platform Stations (HAPSs), where Optical Feeder Links can enable them to provide connectivity to large numbers of users across extensive ground areas. These networks offer some of the advantages of satellites at a lower cost and with higher flexibility.
4. Airplane connectivity: Space lasercom may become instrumental in providing high-speed Internet connectivity to airplanes through Optical Feeder Links to connect aircraft with satellite constellations. With ever-increasing air traffic, this technology will unlock new possibilities for in-flight communication and services for passengers.
5. Terrestrial connections: FSOC will provide readily deployable horizontal links for terrestrial connections, enhancing network capabilities in a flexible manner. These links can be swiftly established where necessary to meet changing connectivity requirements, such as in disaster scenarios.
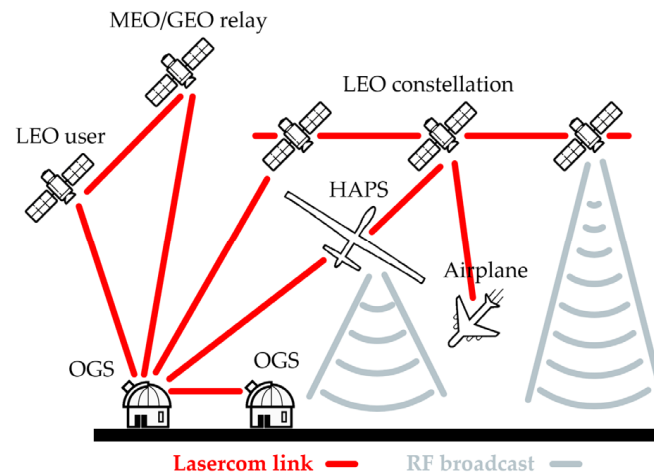
Figure 2. Potential candidate application scenarios for FSOC in B5G.

3. Lasercom Terminal as Fundamental Building Block

Central to the success of FSOC in all of the scenarios described in the previous section is the concept of laser-communication terminal as the fundamental building block. While numerous lasercom terminals had been developed in the past, including several at the NICT, an overly mission-oriented approach often led to a discontinuation of technology development after each mission concluded. The design of traditional lasercom-terminals used to be optimized for a specific mission, posing challenges for adaptability to different conditions, and often requiring costly redesign or customization when requirements evolved. This practice impeded the advancement of realistic and feasible solutions for actual communication scenarios, which could vary from the demonstration environment, delaying their practical deployment to solve specific market needs.

To solve this problem, the NICT has started the development of a series of versatile lasercom terminals with the goal of being capable of fitting a variety of requirements through their internal adaptive operation as well as the selection of their constituent parts between two types of optical heads and two types of modems (see Figure 3) [21]. The fundamental configuration is defined by choosing either the ST (Simple Transponder) or FX (Full Transceiver) type, depending on the basic conditions of operation. The communication requirements can then be further refined by choosing between a 10G-type (10 Gbit/s or below) and a 100G-type modem (100 Gbit/s and above, until the Tbit/s regime with WDM). Lastly, when the fundamental terminal setup for a certain platform or scenario has been established, the terminal itself can adjust its performance to the changing link conditions using internal adaptive techniques. Miniaturization has driven the design of these terminals in order to minimize the impact in terms of size, weight, and power (SWaP) (see Figure 4).

The FX terminal (Figure 5) is the most complete solution suited for applications requiring, in general, some optimum combination of long-distance, high-speed, and bidirectional links [22]. It allows the implementation of stressed scenarios, such as high-speed bidirectional LEO-to-LEO intersatellite links in satellite constellations, ultra-high-speed bidirectional links for HAPS scenarios, or moderate-speed ultra-long-distance links for LEO-GEO. This performance can be achieved in such a small terminal mainly thanks to its 9 cm telescope, which allows a high collimation of its transmitted beams with minimal divergence for optimum transmitted power delivery to the counterpart, while showing a large receiving gain for the receive channel to close the link with enough margin.
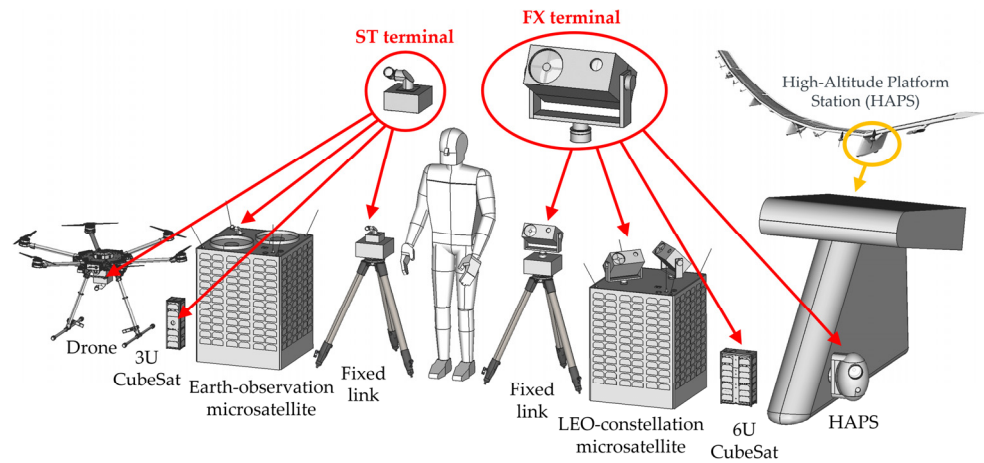
Figure 3. CAD illustration of the 2 types of lasercom terminals fitting multiple platforms.
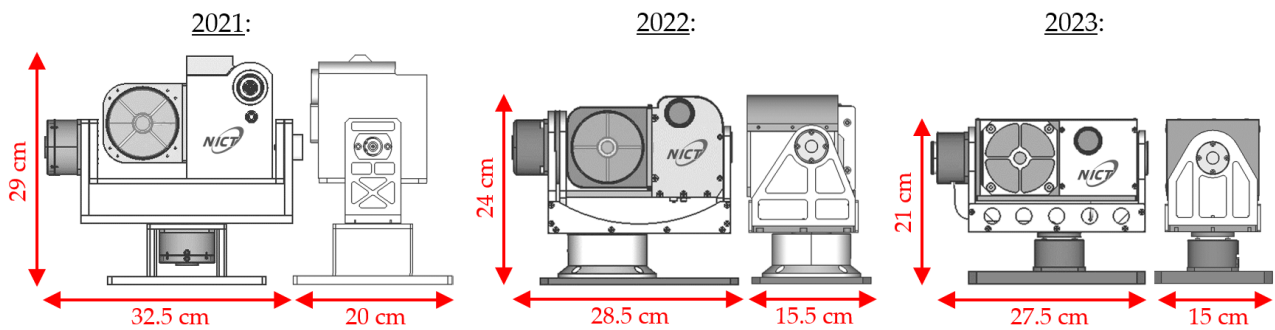

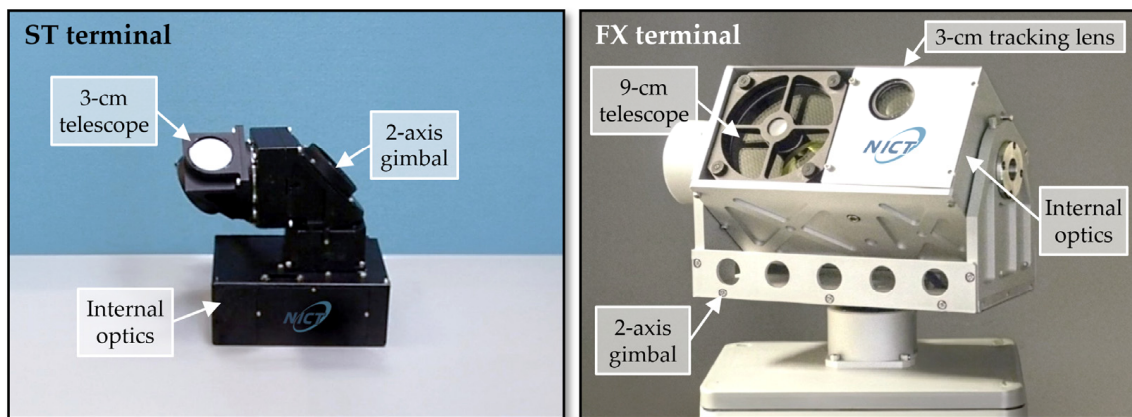**Figure 4.** Miniaturization evolution of the FX terminal over the past 3-year period: 2021–2023.

Figure 5. First functional prototypes of ST (**left**) and FX (**right**) terminals' optical head assemblies.

Conversely, the ST terminal (Figure 6) represents an even further miniaturized version of essentially the same terminal configuration as the FX. It is specifically designed for applications where some of the aforementioned requirements can be relaxed to some extent. For instance, many Earth observation LEO satellites primarily transmit data to the ground, necessitating only a small optical aperture for beam collimation to achieve high-speed transmission and moderate-speed reception. Similarly, in scenarios with shorter distances, such as communication between aircraft, like airplanes, HAPSs, or drones [23], and the ground, the ST terminal's small aperture is adequate to establish ultra-high-speed links even for the received signals, or high-speed bidirectional links over moderate distances.
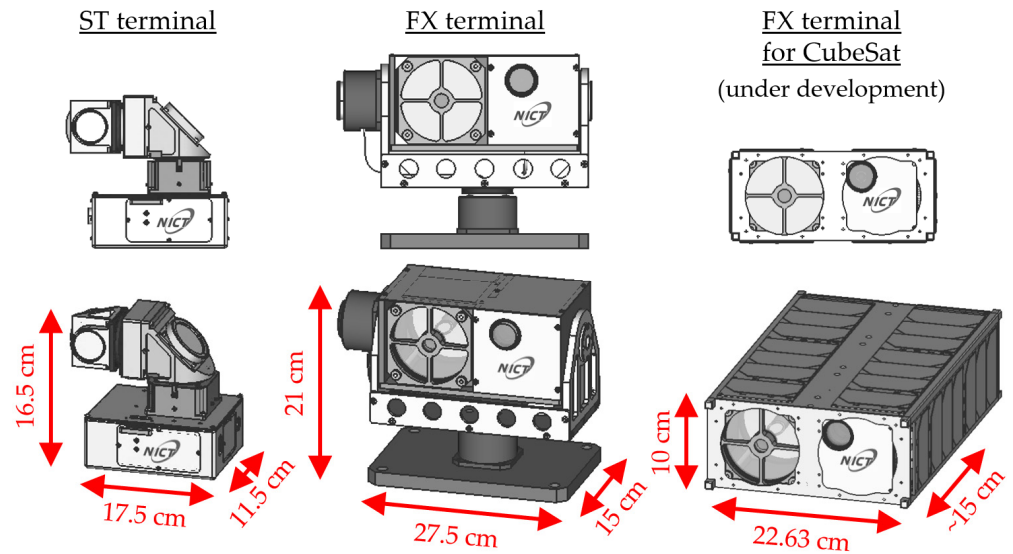
Figure 6. CAD models of the ST (**left**) and FX (**center** and **right**) terminals' optical heads.

In Table 1, an estimation of how each terminal fits the main target scenarios is presented. In cases where the terminal is in a LEO or onboard a HAPS, the maximum transmitted power is 2 W (see Section 4), and it is 3 W when the FX/ST terminals are used on the ground (in horizontal links and with HAPS). The ground stations' and GEO's EDFAs transmit at 10 W. Unless otherwise stated, bidirectional links are assumed, and in those cases, the same terminal is assumed at both ends for simplicity, although multiple combinations of FX and ST are possible. In general, ST can address the same scenarios as FX at the cost of some performance degradation, with the exception of LEO-GEO, where the ST's transmitting and receiving gain are not enough to close the link in any case. With regard to link distance and bitrate, the maximum distance and maximum bitrate are assumed with consideration of the worst case of each scenario. In all these use cases, bitrates are achievable by the NICT's 10G and 2T modems (see Section 4), except for the horizontal link, where there is a sufficient margin to consider a throughput in excess of 2 Tbit/s. In this case, the maximum channel capacity achievable by the terminals' optics in relation to WDM (see Section 4) is assumed.

**Table 1.** Estimation of terminal capabilities to address main target scenarios.

Scenario	Terminal	Distance	Bitrate	Comment
LEO-LEO	FX	5000 km	1 Gbit/s	Sparse const. (long distance)
LEO-LEO	FX	1000 km	10 Gbit/s	Dense const. (short distance)
LEO-GEO	FX	36,000 km	100 Mbit/s	Return link (LEO→GEO)
LEO-GEO	FX	36,000 km	1000 Gbit/s	Forward link (GEO→LEO)
LEO-HAPS	FX	1000 km	10 Gbit/s	Bidirectional (FX↔FX)
HAPS-HAPS	FX	200 km	2 Tbit/s	5 × 400G channels (WDM)
HAPS-OGS	FX	200 km	2 Tbit/s	5 × 400G channels (WDM)
LEO-OGS	FX	1000 km	400 Gbit/s	Downlink (LEO→OGS)
LEO-OGS	FX	1000 km	10 Gbit/s	Uplink (OGS→LEO)
LEO-LEO	ST	1000 km	100 Mbit/s	Dense const. (short distance)
LEO-OGS	ST	1000 km	10 Gbit/s	Downlink (LEO→OGS)
LEO-OGS	ST	1000 km	1 Gbit/s	Uplink (OGS→LEO)
LEO-HAPS	ST	1000 km	100 Mbit/s	Bidirectional (ST↔ST)
HAPS-HAPS	ST	200 km	100 Gbit/s	Bidirectional (ST↔ST)
HAPS-OGS	ST	200 km	100 Gbit/s	Bidirectional (ST↔ST)
Horizontal	FX/ST	20 km	5.6 Tbit/s	14 × 400G channels (WDM)

Figure 6 displays the 3D models of the optical heads corresponding to the final versions of both the ST and FX terminals. On the right-hand side, a CubeSat version of the FX is also depicted. This particular terminal is currently in its final design phase and its design is primarily derived from the FX terminal, with the exception of the gimbal system. The flight

version will be manufactured in 2024 to be space qualified and delivered to the launcher in 2025.

4. Lasercom Terminal Characteristics

This section gives an outline of the basic characteristics and technologies of the FX/ST lasercom terminals. While both terminals exhibit distinct external appearances, they share the same basic internal configuration (see Figure 7). The two terminals have coarse-pointing systems based on 2-axis gimbals with a pointing resolution of ~30 µrad controlled by wide-field-of-view detectors (C-PSD) to quickly close the control loop acquiring the counterpart terminals. Regarding optics, the transmitter's subsystems incorporate a point-ahead mechanism (PAM) for scenarios involving long distances and narrow beam divergence. This mechanism accounts for the angular separation between the transmitted and received beams due to the finite speed of light. Additionally, it can compensate for deviations of the optical axis in real time by monitoring the transmitted signal's position using the point-ahead sensor (PAS). The receiver's subsystems are equipped with a fine-pointing mechanism (FPM) to allow for single-mode fiber coupling governed by narrow-field-of-view tracking detectors (F-PSD). PAM and FPM are both based on microelectronic mechanical systems (MEMS) for size optimization and are currently being customized to handle high optical power (several Watts) in a vacuum environment with minimal surface distortion to avoid wavefront errors.
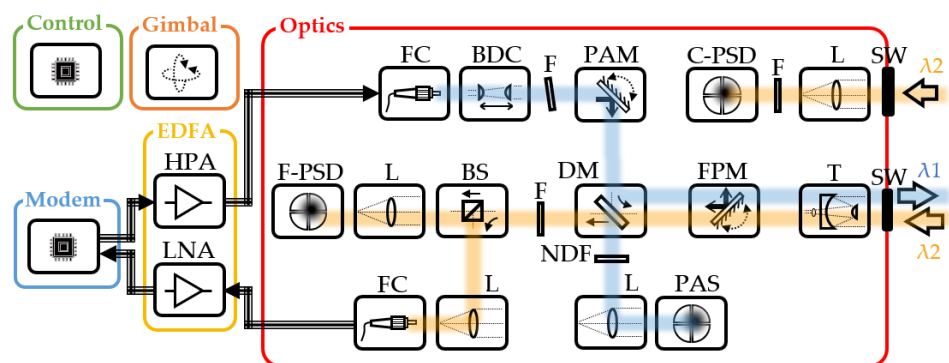
SW = Solar Window; **L** = Lens; **F** = Filter; **T** = Telescope; **DM** = Dichroic mirror; **BS** = Beam Splitter; **FC** = Fiber Connector; **NDF** = Neutral-Density Filter; **BDC** = Beam-Divergence Control; **FPM** = Fine-Pointing Mirror; **PAM** = Point-Ahead Mirror; **PAS** = Point-Ahead Sensor; **PSD** = Position-Sensitive Detector; **C-PSD** = Coarse PSD; **F-PSD** = Fine PSD; **HPA** = High-Power Amplifier; **LNA** = Low-Noise Amplifier

Figure 7. FX terminal's block diagram, including optical, electrical, and mechanical systems.

Figure 7 shows the basic block diagram of the FX terminal, including the optical, electrical, and mechanical systems. The ST terminal's block diagram is essentially the same as that of the FX terminal but without the coarse-pointing assembly (C-PSD + F + L + SW) because of the single optical aperture. Instead, the ST terminal implements both coarse- and fine-pointing functions within the same optical path but divides the received signal toward two PSDs with different fields of view according to the needs of the C-PSD and F-PSD. Since this technique is 3 dB less efficient because of the beam division, both PSDs are being planned to be replaced by a single miniaturized FPA (Focal Plane Array) working as a common tracking detector, which is currently under development. Besides overcoming the 3 dB penalization, it will allow for an increase in sensitivity as well as dynamic range, both by several tens of dB. After being proven in the ST terminal, the same technique will be replicated in the FX terminal, resulting in identical block diagrams for both terminals. The different telescopes and equivalent internal optics are depicted in Figure 8.
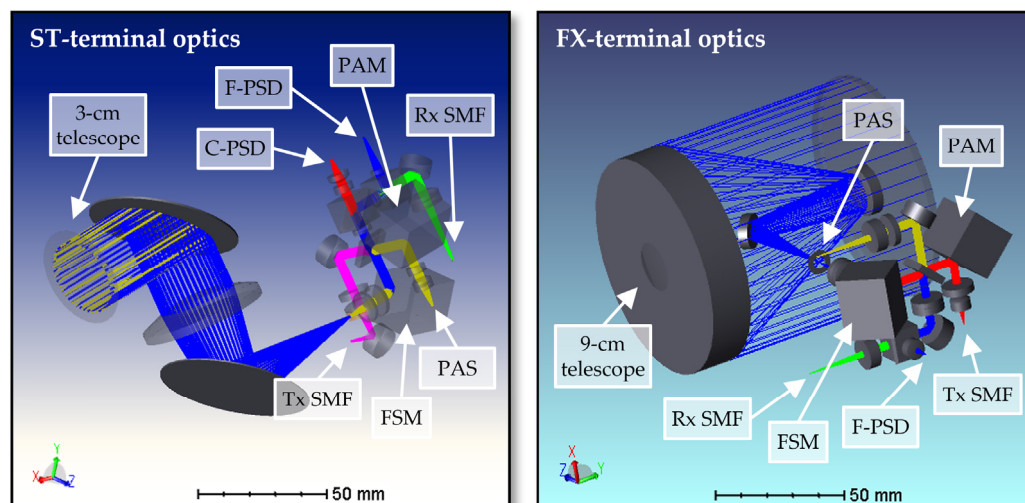
Figure 8. Three-dimensional layout of the optical systems of the ST (**left**) and FX (**right**) terminals.

Lastly, it is worth mentioning the effort put into developing a miniaturized gimbal for the ST, which is the most compact gimbal integrated into a terminal known to date. This was achieved by combining the telescope with the gimbal, unlike the usual technique of using a periscope within the gimbal and a telescope behind it within the internal optics. In this case, by installing the output lens inside the gimbal, the overall size is reduced because the beam size is already minimized when it reaches the internal optics.

A key feature of the FX/ST terminals is the inclusion of a beam-divergence control (BDC) system [24]. This device was custom developed in collaboration with Tamron Co, Ltd. [25], with the goal of increasing the flexibility of operation, and it will be the world's first BDC system integrated in a lasercom terminal. It allows the transmission of a collimated beam with minimal divergence as well as increases the angle to be wider by up to ~20 times, reaching the mrad regime. Among the advantages of the BDC, it is worth mentioning the capability to optimize beam divergence according to the actual operation conditions, such as link distance, pointing error, and vibration environment. For example, it can speed up the acquisition procedure by widening the first light's divergence angle or enhance link availability when there is a significant variation in the distance range. To optimally utilize this capability, it is necessary for the tracking detector to have a very wide dynamic range and high sensitivity. The future integration of the FPA instead of the conventional PSD, introduced in the previous paragraph, will meet this requirement, allowing the terminals to detect extremely low power levels corresponding to the initial acquisition with wide divergence, while simultaneously operating with power levels several tens of dB higher during the communication phase with narrower beams.

Figure 9 shows the final device's appearance after extensive miniaturization efforts, resulting in a size not much larger than that of a conventional fixed collimator. Both terminals share the same BDC device because, although each terminal is typically targeted for different distance ranges (longer in the case of the FX compared to the ST), the ~3 mm beam produced by the BDC is expanded to different output optical signals with the different telescopes in the ST and FX, while also achieving different beam-divergence ranges according to each terminal's requirements. Additionally, to maintain optical-axis stability when modifying the beam divergence or with temperature changes, the optical signal transmitted by the BDC is monitored by the PAS and corrected by the PAM in real time.
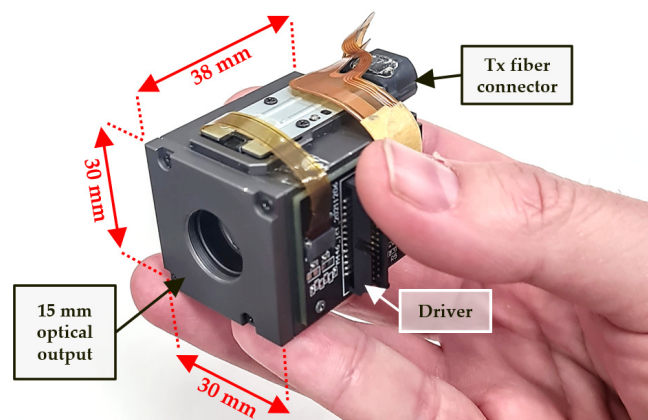
Figure 9. Beam-divergence control (BDC) device.

The main difference between the FX and ST terminals is the telescope's optical aperture size (aside from the gimbal design, which is a consequence of the telescope's design). The FX terminal includes a 9 cm miniaturized telescope, which allows the transmission of a narrow laser beam to cover long distances as well as provides a high receiving gain to close the bidirectional links at high speed. In contrast, the ST terminal exhibits a smaller size at the cost of sacrificing some performance compared to the FX terminal. However, the optics of both terminals are designed to maximize the throughput, when necessary, by employing WDM (Wavelength-Division Multiplexing). Two bands, comprising 1535–1545 nm and 1555–1565 nm, with an intermediate band wide enough for tx/rx isolation purposes, enable the use of up to 14 channels per band when considering the DWDM ITU channel grid. This offers a potential bidirectional throughput in the order of 5 Tbit/s assuming 400 Gbit/s per channel.

The FX/ST terminals are designed to be combined with two types of modems to offer increased flexibility when selecting the appropriate combination for a specific application. Currently, the primary solution is the 10G modem (see Figure 10), whose development has already been completed. This modem incorporates bit interleaving and error correction to achieve error-free communications in various conditions including atmospheric turbulence. The interleaver time exceeds 10 ms, and the Forward Error Correction (FEC) is Reed–Solomon error correction, with two different code rates to select: 1/2 (50%) or 7/8 (~90%). The communication format is based on intensity modulation and direct detection (IM/DD), allowing for data rate adjustments to match the link conditions. The Variable Data Rate (VDR) system permits communication speeds ranging from 10 Gbit/s to 0.6 Gbit/s (with an upcoming extension down to 0.1 Gbit/s). By changing the data rates, the number of photons per bit can be increased to improve sensitivity. Ideally, a span as wide as {100 Mbit/s–10 Gbit/s}, as in the case of this modem, should provide a dynamic range of up to 20 dB, which allows the optimization of the modem's behavior according to the actual channel conditions.

The 10G modem supports several communication modes: a test mode for transmitting pseudorandom binary sequences (PRBSs) to analyze the bit error rate (BER); an Ethernet mode for standard 10GBASE-T data exchange by using an additional Ethernet port for the communication signals; an SSD mode for transmitting data stored in the internal 1 TB memory and storing the received data (which is particularly well suited for applications where data production and transmission are decoupled such as in Earth observation LEO satellites or in single-terminal relays); and a relay mode for looping back processed data upon receipt. This modem has been custom developed in a single electronic board to keep the high-speed electrical connections as short as possible, and its dimensions are compatible with the 6U CubeSat's form factor (9.5 × 22 cm).

Currently, another experimental modem is in the research and development phase, aiming at achieving significantly higher speeds than the 10G modem. An initial prototype has been manufactured in a compact form factor (a single board of 20 × 20 cm) to enable its

use in field experiments (see Figure 11). This prototype can achieve 2 Tbit/s by employing WDM with five channels, each operating up to 400 Gbit/s, which makes it the world's smallest Tbit/s class modem. This prototype offers the flexibility to adjust the data rate on a per-channel basis, with options of 100, 200, or 400 Gbit/s, resulting in a selectable throughput ranging from 100 Gbit/s to 2 Tbit/s to adapt to the actual channel conditions. Since this modem is based on the more efficient coherent format, data rate adjustments are achieved by changing the modulation between 16QAM (100 Gbit/s), 8QAM (200 Gbit/s), and QPSK (400 Gbit/s).
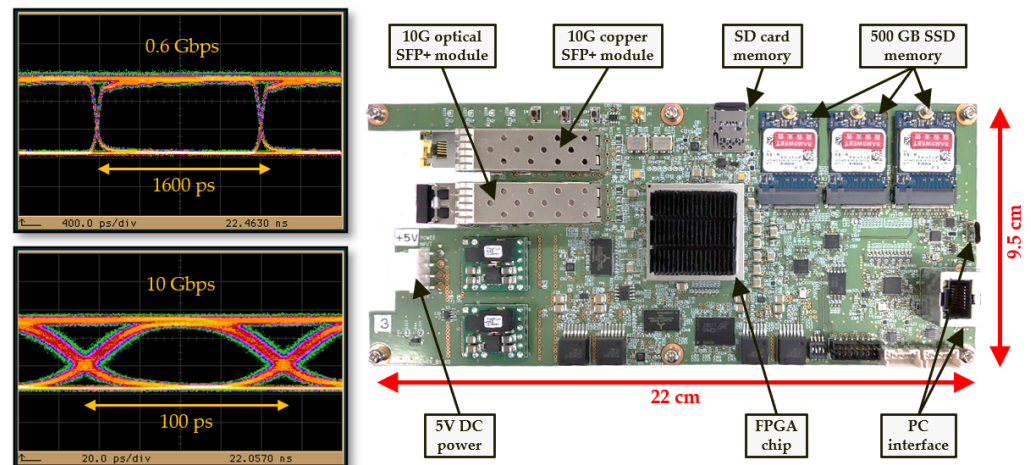
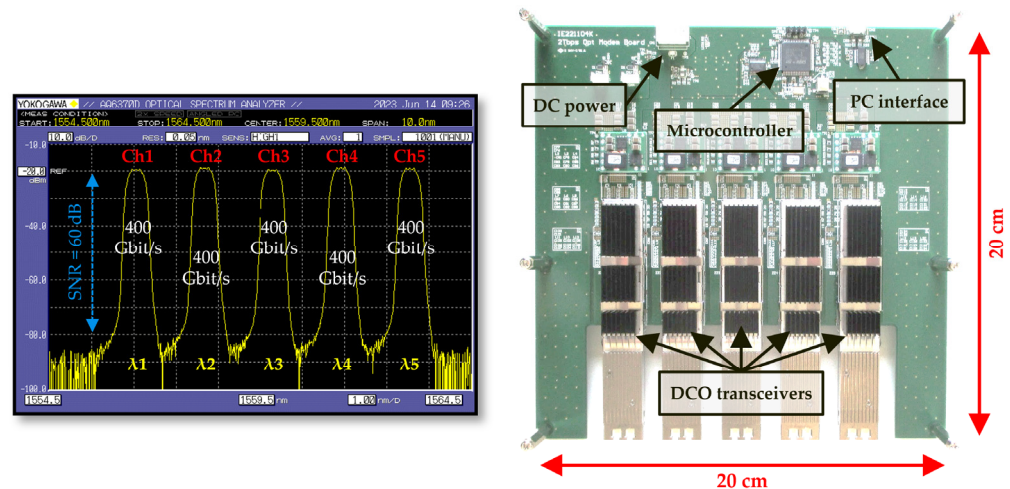**Figure 10.** Eye diagrams of 0.6 Gbit/s and 10 Gbit/s (**left**), and 10G modem board (**right**).

Figure 11. Spectrum of 5 × 400 Gbit/s channels (**left**) and 2 Tbit/s modem board (**right**).

This prototype currently supports the transmission of PRBS + BERT exclusively, which is aimed at understanding the optimal error protection processing required for communications at such high speeds. Error correction coding is based on oFEC (openFEC), which provides a net coding gain of over 10 dB for BER = 10^{-15} in response to a pre-FEC BER threshold of 10^{-2}. After experimental tests that will help understand the specific requirements related to atmospheric propagation at an ultra-high speed and with coherent detection, the full version of the modem will be developed, including data transmission.

The use of digital coherent optics (DCO) to support bitrates of 100 Gbit/s and above influenced the decision to rely solely on wavelength to discriminate the transmission and reception paths in the terminals, rather than relying on polarization as in the initial design. This update is due to DCO's ability to double the speed by utilizing two orthogonal polarizations, a functionality that was incompatible with the initial design. As a result of this design change, the terminals are also compatible with quantum communications, as

they allow the transmission and preservation of polarization in both the transmission and reception paths.

A series of compact optical amplifiers (EDFAs) were developed for integration with the terminals, conforming to the CubeSat 1U form factor standard. Two versions were designed, with the initial version completed in 2020 including a 2-W High-Power Amplifier (HPA). The details of this amplifier have been presented in [26], and its 3D model and a picture of it being mounted on a 3U CubeSat is shown in Figure 12 (left). This miniaturized EDFA successfully passed full space environment qualification, including the ISO 19683:2017 and ISO 15864:2004 standards for vibration, shock, thermal vacuum, and radiation tests. In 2023, a second version (Figure 12, right) was completed, incorporating a Low-Noise Amplifier (LNA) in addition to the 2-W HPA in order to support bidirectional links. At the time of writing this article, the second version is undergoing the space environment tests.
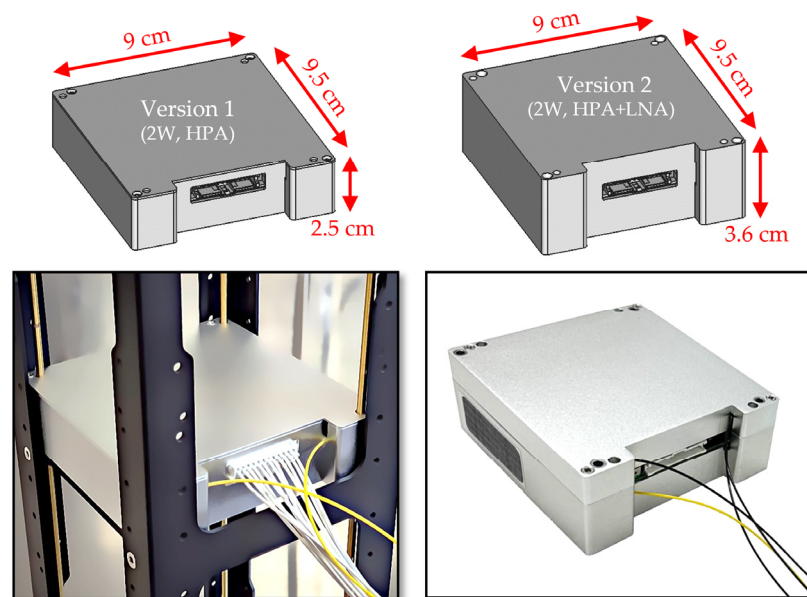

Figure 12. Miniaturized CubeSat's EDFA version 1 (**left**) and version 2 (**right**).

The LNA section includes a spectral filter of 1 nm to remove the ASE noise to preserve the OSNR (Optical-Signal-to-Noise Ratio). Although a narrower filter could be employed, this spectral width was selected as a compromise to contain, without losses, all the Doppler shifts in the worst-case scenario of a LEO satellite, avoiding the necessity of employing a sophisticated wavelength compensation system. The EDFA version 2 maintains the ultra-compact size of the first version, with the same dimensions (CubeSat compatible) and only 11 mm of additional height, being the world's smallest space-grade HPA + LNA EDFA to the authors' knowledge. All the other characteristics are inherited from version 1, and in this case, both sections, HPA and LNA, can be controlled independently to allow more energy-efficient use of the EDFA in cases where only one is necessary. Both versions will be launched onboard two different 6U CubeSats within the next 1–2 years for in-orbit experiments.

5. Terminals' Validation and Demonstration Plans

Currently, demonstrations for a wide variety of scenarios employing these lasercom terminals are under preparation. These scenarios encompass communication using satellites, HAPS, airplanes, and fixed points. At the time of writing this article, the final characterization of the terminals, as well as the last laboratory tests, are in the process of nearing completion. Simultaneously, the terminals' control system is being finalized to enable automated operation with minimal telemetry/telecommand intervention. In the flat-sat laboratory test of the FX terminal with the 10G modem (see Figures 13 and 14), a receiver's

sensitivity of -43.3 dBm could be confirmed at 10 Gbit/s for BER $\approx 10^{-3}$ before FEC with an LNA pre-amplification. Under the same conditions but without pre-amplification, the modem shows a sensitivity of -32.6 dBm.
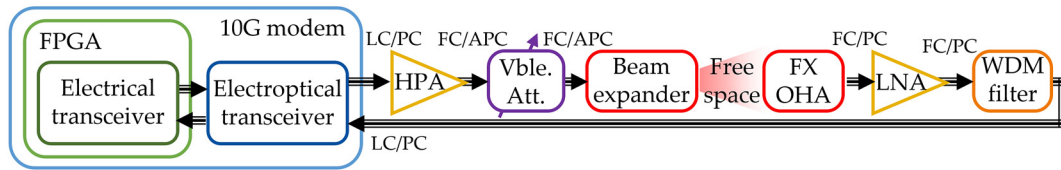

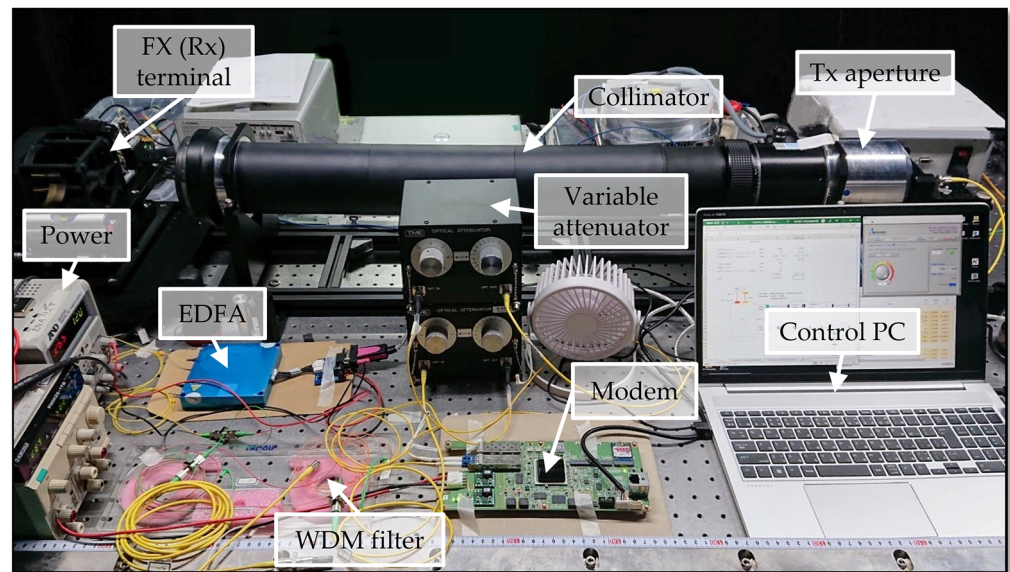**Figure 13.** Block diagram of the flat-sat test for the FX terminal's communication system.

Figure 14. Laboratory picture of the flat-sat test for the FX terminal's communication system.

A similar sensitivity characterization was carried out for the 2 Tbit/s modem prototype (see Figure 15), obtaining a maximum sensitivity of -36.9 dBm without pre-amplification for the case of 100 Gbit/s per channel (using QPSK modulation with coherent detection), while in this case, the measurements were taken after FEC, which was integrated into the optical transceivers. This is the optimum case for the 2 Tbit/s modem because, for higher data rates, QAM modulation, which exhibits a higher BER under the same conditions, must be used. For example, for 16QAM to produce 400 Gbit/s per channel, the sensitivity is -21.9 dBm.
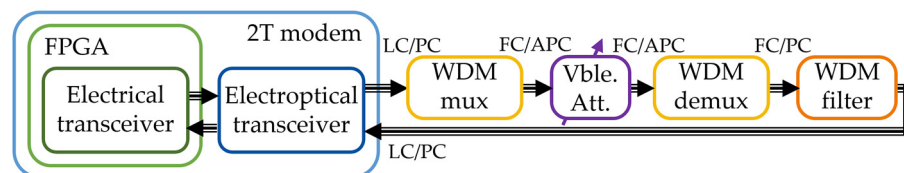

Figure 15. Block diagram of the 2 Tbit/s modem prototype's performance test.

The performance of the pre-amplified case will be characterized in the near future, as well as the dependence on the OSNR. Based on the current measurements and the expected performance, it can be foreseen that the 400 Gbit/s case will be quite challenging because, even though the LNA can help improve sensitivity, the required OSNR of the 16QAM 400 Gbit/s case is expected to be over 10 dB higher than the QAM 100 Gbit/s case. Therefore, the operational model of the Tbit/s modem will require accurate channel estimation to optimize its performance according to the present channel state information (CSI).

In order to demonstrate the versatility of the ST/FX terminals, all scenarios described in Section 2 as the most promising applications for FSOC to be applied in 5G networks are currently in preparation. In ascending order of complexity, the first of these scenarios, i.e., terrestrial connections (see Figure 16), is taking place at the time of writing this manuscript. It involves an 8 km horizontal experiment between the NICT headquarters in Tokyo (Koganei) and a nearby university campus, utilizing both the 10G and 2T modems. This experiment will verify all the basic communication functions of the terminals, including pointing and tracking capabilities, beam-divergence management, fiber coupling under atmospheric turbulence, and 1–10 Gbit/s data rates, amongst others, and a vibration stage will be used to emulate the conditions experienced by airborne and satellite platforms.
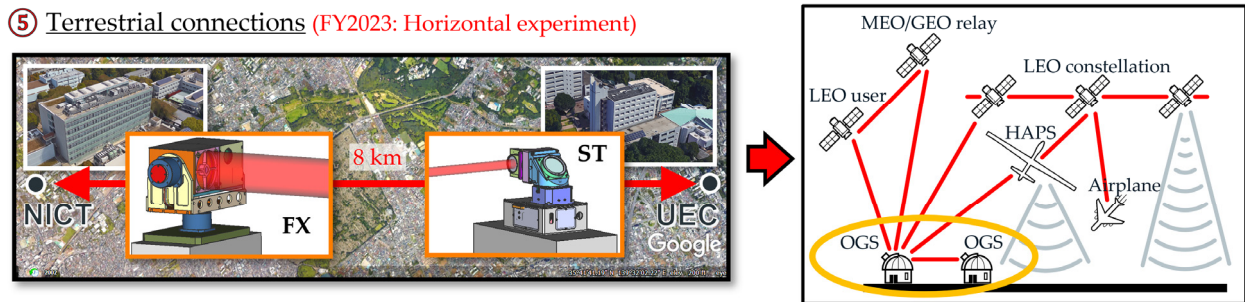

Figure 16. The terminals' demonstration plan in relation to the 5th scenario described in Section 2.

Figure 17 displays the preliminary result of the 8 km horizontal experiment carried out in Tokyo during February 2024. The figure presents two examples of pre-FEC quasi-error-free transmission at 10 Gbit/s. FEC performance could be confirmed, achieving error-free transmission, but interleaving capability is currently being adjusted in order to remove the occasional burst errors. Multiple data rates were confirmed during the experiment, ranging from 0.6 to 10 Gbit/s. These measurements show the fiber-coupled power just before the FX's modem input. To illustrate the variable influence of atmospheric turbulence, measurements corresponding to different times of the day are shown—during the day on the left-hand side and during the night on the right-hand side—showing almost 3 dB of additional scintillation in the daytime case. The camera images of the received beam clearly illustrate the impact of atmosphere on the transmitted beam depending on the turbulence conditions.
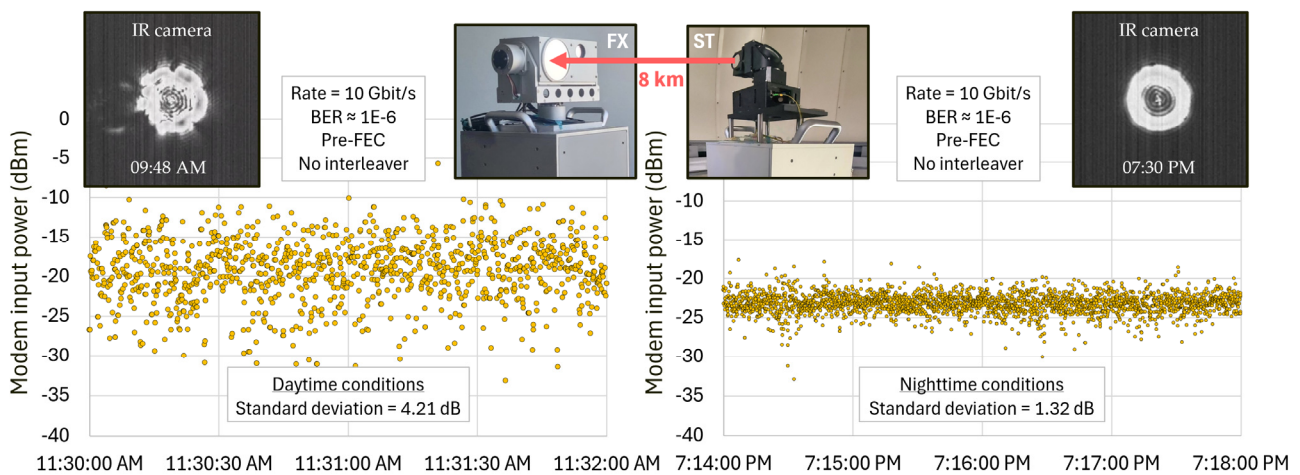

Figure 17. Horizontal link result showing 10 Gbit/s transmission during day (**left**) and night (**right**).

Additionally, and due to the specific characteristics of these kinds of fixed links, the design of a highly simplified version of the terminals is under consideration. This version will exclude gimbals and high-power EDFAs, which will significantly reduce power

consumption. Whether fixed or gimballed, another application with plans for mid-term demonstration includes using the terminals as intermediate nodes, thus playing the role of relaying stations to extend the total range where there is no direct line of sight. By design, these terminals offer the possibility to select between two different operating principles when serving as relays: (1) optical-to-electrical and electrical-to-optical conversion by using the relay mode of the 10G modem, and (2) all-optical relay. The first principle implies demodulating and decoding the received signal, which benefits from the interleaver and error-correction functions. The second principle implies regenerating the received signal in the optical domain by using the same signal after the receiving LNA to feed the transmitting HPA, which does not allow error correction but can benefit from a better overall performance [27].

The subsequent step (see Figure 18) will involve mounting the ST terminal on an aircraft and implementing a compact ground station based on the FX terminal to demonstrate the complete functionality of both terminals, including high-speed acquisition, pointing, and tracking, as well as communications in a realistic scenario with mobile platforms affected by atmospheric conditions and a realistic vibration environment. The authors had already carried out a similar experiment using a Cessna aircraft for the evaluation of an RF array antenna in 2021 [28], and the plan is to replicate it with the ST terminal instead. Based on the previously employed interface with the airplane, the expected field of regard of the ST terminal is about 45° relative to the nadir, which makes a maximum slant path of 1.4 km assuming a flight altitude of 1 km. There are plans to replicate this experiment afterwards using the HAPS in order to test for significantly longer distances as well as under harsher environmental conditions: At an altitude of 20 km, the pressure is about 5% of the ground's pressure, and the temperature is about −60 °C.
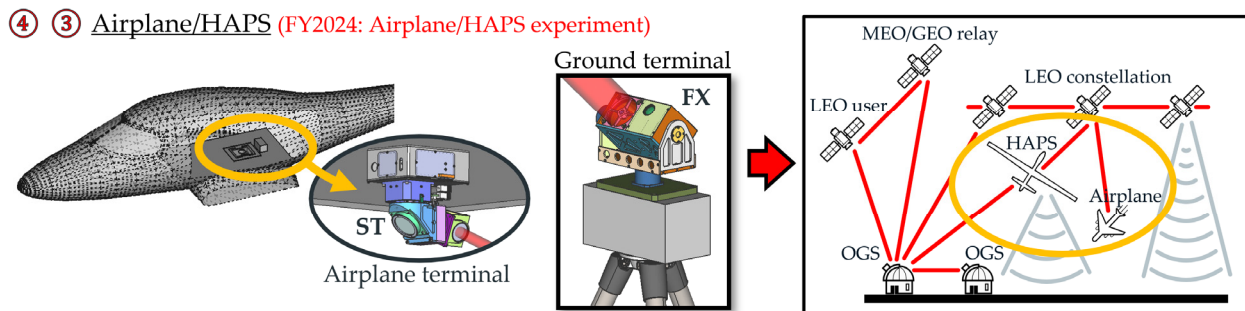
④ ③ Airplane/HAPS (FY2024: Airplane/HAPS experiment)

Figure 18. The terminals' demonstration plan in relation to the 3rd and 4th scenarios described in Section 2.

The CubeSat version of the FX terminal had already been designed, with minor differences relative to the original FX terminal, such as the absence of the gimbal and related electronics and the RF subsystem. This terminal is currently under development, with plans to be launched onboard a 6U CubeSat during the Japanese fiscal year 2025. This mission is named CubeSOTA [29], which will continue the legacy of the successful NICT's SOTA [15], and it is aimed at demonstrating various scenarios, including LEO–ground, LEO-HAPS, and LEO-LEO. CubeSOTA will be the first in-orbit validation of the terminals presented in this manuscript (see Figure 19). As an unprecedented technological challenge, it is worth highlighting that CubeSOTA aims to demonstrate the most efficient optical transmission to date from a CubeSat, with a beam divergence several times narrower than previous experiments owing to the use of the FX's 9 cm telescope.
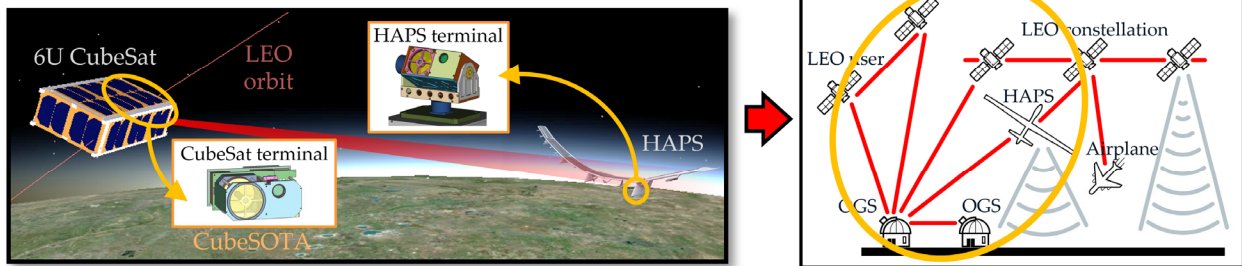
Figure 19. The terminals' demonstration plan in relation to the 2nd scenario described in Section 2.

Lastly, under the NICT's B5G Function Realization Program [30], a version adapted for LEO constellation is being designed based on the FX terminal with the goal of integration and deployment within the Axelspace's Earth observation satellite constellation [31]. The plan includes implementing five lasercom terminals per 100 kg class satellite (two for intraplane ISL, two for interplane ISL, and one for LEO–ground or LEO–user) in a Walker constellation of 20 orbital planes and 20 satellites per plane (see Figure 20). LEO satellite constellations represent the FSOC application that has gained the most acceptance in the telecommunications market, as highlighted by SpaceX's Starlink [32] and the upcoming deployment of multiple additional constellations [33,34]. Among their main advantages is the potential for global connectivity with lower delay compared to traditional optical networks [35]. When combined with the AI management of the multiple parameters that lasercom terminals and other network elements allow [36], they promise to offer an innovative solution for global connectivity.

Figure 20. The terminals' demonstration plan in relation to the 1st scenario described in Section 2.

6. Conclusions

In 2024, the NICT plans to finalize the first fully functional prototypes of miniaturized laser communication terminals for various platforms, offering adaptability to diverse scenarios where free-space optical communications can enhance B5G networks and other applications. This paper presents an overview of the purpose of these terminals and what needs they have been designed to address, their capabilities, their constituent technologies, and demonstration plans.

In particular, in the context of B5G/6G networks, where increasing bandwidth and reducing latency are critical, a key challenge has been identified: creating a versatile and superior solution to provide wireless support in moderate-distance environments where delays are comparable to or shorter than those of fixed networks while minimizing size, weight, and power impact compared to current alternatives. The communication terminals developed by the NICT meet these requirements while allowing the possibility of reuse in a variety of applications and diverse platforms without customization.

The manuscript introduces several innovations integrated into the terminals, such as the manufacture of the smallest miniaturized EDFA with integrated HPA and LNA to date, the first-ever integration of a beam-divergence control system in a practical communication

terminal, the development of the most compact Tbit/s-class modem prototype documented in the literature, and the smallest gimbal design integrated in a lasercom terminal.

The creation of two types of terminals and two types of modems also offers the possibility of finding a versatile solution for each scenario + platform. This adds to the adaptability that each terminal + modem configuration provides due to their capability of dynamically accommodating multiple variable parameters, such as beam divergence, transmission speed, error correction, transmitted power, or optical-axis alignment, which, in the future, can additionally be governed by AI in real time.

The demonstration plans for a wide variety of scenarios employing these terminals are presented, including the laboratory characterization of their constituent parts as well as the complete terminals, preliminary results from the first experimental validation in a realistic environment with an 8 km horizontal link, and the immediate plans to demonstrate scenarios involving airplane, HAPS, and satellite platforms.

The objective of these demonstrations is not only to prove that the terminals can fulfill their purpose in various scenarios but also to ensure they can be reliably used as elements integrated in communication networks. This validation is particularly critical for their practical use to become a reality and has been identified as the main unresolved issue in certain applications, especially those related to atmospheric links.

References

1. Council for Science, Technology and Innovation, Cabinet Office, Government of Japan. Report on the 5th Science and Technology Basic Plan. 18 December 2015. Available online: https://www8.cao.go.jp/cstp/kihonkeikaku/5basicplan_en.pdf (accessed on 25 April 2024).
2. National Institute of Information and Communications Technology. Beyond 5G/6G White Paper. June 2023. Available online: https://beyond5g.nict.go.jp/images/download/NICT_B5G6G_WhitePaperEN_v3_0.pdf (accessed on 25 April 2024).
3. Tong, W.; Zhu, P. *6G: The Next Horizon: From Connected People and Things to Connected Intelligence*; Cambridge University Press: Cambridge, UK, 2021. [CrossRef]
4. Jiang, W.; Han, B.; Habibi, M.A.; Schotten, H.D. The Road Towards 6G: A Comprehensive Survey. *IEEE Open J. Commun. Soc.* **2021**, *2*, 334–366. [CrossRef]
5. Viswanathan, H.; Mogensen, P.E. Communications in the 6G era. *IEEE Access* **2020**, *8*, 57063–57074. [CrossRef]
6. Saad, W.; Bennis, M.; Chen, M. A Vision of 6G Wireless Systems: Applications, Trends, Technologies, and Open Research Problems. *IEEE Netw.* **2020**, *34*, 134–142. [CrossRef]
7. Chowdhury, M.Z.; Shahjalal, M.; Ahmed, S.; Jang, Y.M. 6G Wireless Communication Systems: Applications, Requirements, Technologies, Challenges, and Research Directions. *IEEE Open J. Commun. Soc.* **2020**, *1*, 957–975. [CrossRef]
8. Carrasco-Casado, A.; Mata-Calvo, R. Space Optical Links for Communication Networks. In *Springer Handbook of Optical Networks, Springer Handbooks*; Mukherjee, B., Tomkos, I., Tornatore, M., Winzer, P., Zhao, Y., Eds.; Springer: Cham, Switzerland, 2020; pp. 1057–1103. [CrossRef]
9. Cao, X.-Y.; Li, B.-H.; Wang, Y.; Fu, Y.; Yin, H.-L.; Chen, Z.-B. Experimental quantum e-commerce. *Sci. Adv.* **2024**, *10*, eadk3258. [CrossRef] [PubMed]

10. Pirandola, S. Satellite quantum communications: Fundamental bounds and practical security. *Phys. Rev. Res.* **2021**, *3*, 023130. [CrossRef]
11. Xie, Y.-M.; Lu, Y.-S.; Weng, C.-X.; Cao, X.-Y.; Jia, Z.-Y.; Bao, Y.; Wang, Y.; Fu, Y.; Yin, H.-L.; Chen, Z.-B. Breaking the Rate-Loss Bound of Quantum Key Distribution with Asynchronous Two-Photon Interference. *PRX Quantum* **2022**, *3*, 020315. [CrossRef]
12. Vallone, G.; Bacco, D.; Dequal, D.; Gaiarin, S.; Luceri, V.; Bianco, G.; Villoresi, P. Experimental Satellite Quantum Communications. *Phys. Rev. Lett.* **2015**, *115*, 040502. [CrossRef] [PubMed]
13. Araki, K.; Arimoto, Y.; Shikatani, M.; Toyoda, M.; Toyoshima, M.; Takahashi, T.; Kanda, S.; Shiratama, K. Performance evaluation of laser communication equipment onboard the ETS-VI satellite. In Proceedings of the Free-Space Laser Communication Technologies VIII, San Jose, CA, USA, 27 January–2 February 1996; Volume 2699. [CrossRef]
14. Toyoshima, M.; Takenaka, H.; Shoji, Y.; Takayama, Y.; Koyama, Y.; Kunimori, H. Results of Kirari optical communication demonstration experiments with NICT optical ground station (KODEN) aiming for future classical and quantum communications in space. *Acta Astronaut.* **2012**, *74*, 40–49. [CrossRef]
15. Carrasco-Casado, A.; Takenaka, H.; Kolev, D.; Munemasa, Y.; Kunimori, H.; Suzuki, K.; Fuse, T.; Kubo-Oka, T.; Akioka, M.; Koyama, Y.; et al. LEO-to-ground optical communications using SOTA (Small Optical TrAnsponder)–Payload verification results and experiments on space quantum communications. *Acta Astronaut.* **2017**, *139*, 377–384. [CrossRef]
16. Toyoshima, M. Hybrid High-Throughput Satellite (HTS) Communication Systems using RF and Light-Wave Communications. In Proceedings of the 2019 IEEE Indian Conference on Antennas and Propogation (InCAP), Ahmedabad, India, 19–22 December 2019. [CrossRef]
17. Munemasa, Y.; Saito, Y.; Carrasco-Casado, A.; Trinh, P.V.; Kolev, D.; Takenaka, H.; Suzuki, K.; Kubo-oka, T.; Fuse, T.; Kunimori, H.; et al. Critical Design Results of Engineering Test Satellite 9 Communications Mission: For High-Speed Laser Communication, "HICALI" mission. In Proceedings of the 70th International Astronautical Congress, Washington, DC, USA, 21–25 October 2019. IAC-19-F2.2.3.
18. Kolev, D.; Shiratama, K.; Carrasco-Casado, A.; Saito, Y.; Munemasa, Y.; Nakazono, J.; Trinh, P.V.; Kotake, H.; Kunimori, H.; Kubooka, T.; et al. Preparation of High-Speed Optical Feeder Link Experiments with "HICALI" Payload. In Proceedings of the SPIE Photonics West, San Francisco, CA, USA, 22–27 January 2022; Volume 11993. [CrossRef]
19. Precedence Research. 5G Services Market Size, Growth, Share, Trends Report 2030. Report Code 2108. 2023. Available online: https://www.precedenceresearch.com/5g-infrastructure-market (accessed on 25 April 2024).
20. Grand View Research. 5G Services Market Size, Share & Trends Analysis Report by Communication Type (FWA, eMBB, uRLLC, mMTC), by Vertical (Manufacturing, IT & Telecom, BFSI), by Region (Asia Pacific, North America), and Segment Forecasts, 2023–2030. Report ID: GVR-3-68038-435-2. 2023. Available online: https://www.grandviewresearch.com/industry-analysis/5g-services-market (accessed on 25 April 2024).
21. Carrasco-Casado, A.; Shiratama, K.; Trinh, P.V.; Kolev, D.; Ishola, F.; Fuse, T.; Tsuji, H.; Toyoshima, M. NICT's versatile miniaturized lasercom terminals for moving platforms. In Proceedings of the IEEE International Conference on Space Optical Systems and Applications (ICSOS), Kyoto, Japan, 28–31 March 2022. [CrossRef]
22. Carrasco-Casado, A.; Shiratama, K.; Trinh, P.V.; Kolev, D.; Munemasa, Y.; Fuse, T.; Tsuji, H.; Toyoshima, M. Development of a miniaturized laser-communication terminal for small satellites. *Acta Astronaut.* **2022**, *197*, 1–5. [CrossRef]
23. Trinh, P.V.; Carrasco-Casado, A.; Okura, T.; Tsuji, H.; Kolev, D.R.; Shiratama, K.; Munemasa, Y.; Toyoshima, M. Experimental Channel Statistics of Drone-to-Ground Retro-Reflected FSO Links With Fine-Tracking Systems. *IEEE Access* **2021**, *9*, 137148–137164. [CrossRef]
24. Carrasco-Casado, A.; Shiratama, K.; Kolev, D.; Trinh, P.V.; Fuse, T.; Fuse, S.; Kawaguchi, K.; Hashimoto, Y.; Hyodo, M.; Sakamoto, T.; et al. Prototype Development and Validation of a Beam-Divergence Control System for Free-Space Laser Communications. *Front. Phys.* **2022**, *10*, 878488. [CrossRef]
25. Tamron Co, Ltd. Development of Optics for Satellite Implementation, Optics for Free Space Optical Communication. Available online: https://www.tamron.com/global/technology/detail/20230215003513.html (accessed on 25 April 2024).
26. Carrasco-Casado, A.; Shiratama, K.; Kolev, D.; Trinh, P.V.; Ishola, F.; Fuse, T.; Toyoshima, M. Development and Space-Qualification of a Miniaturized CubeSat's 2-W EDFA for Space Laser Communications. *Electronics* **2022**, *11*, 2468. [CrossRef]
27. Bayaki, E.; Michalopoulos, D.S.; Schober, R. EDFA-Based All-Optical Relaying in Free-Space Optical Systems. *IEEE Trans. Commun.* **2012**, *60*, 3797–3807. [CrossRef]
28. Okura, T.; Kan, T.; Okawa, M.; Takahashi, T.; Tsuji, H.; Toyoshima, M. Demonstration using Cessna Aircraft of Active Electronically Steered Array Antenna for Satellite Communications. In Proceedings of the 72nd International Astronautical Congress, Dubai, United Arab Emirates, 25–29 October 2021. IAC-21-B2.2.8.
29. Carrasco-Casado, A.; Toyoshima, M.; Do, P.X.; Kolev, D.; Hosonuma, T.; Shiratama, K.; Kunimori, H.; Trinh, P.V.; Abe, Y.; Nakasuka, S. Intersatellite link between CubeSOTA (LEO CubeSat) and ETS9-HICALI (GEO satellite). In Proceedings of the IEEE International Conference on Space Optical Systems and Applications (ICSOS), Portland, OR, USA, 14–16 October 2019. [CrossRef]
30. National Institute of Information and Communications Technology. Beyond 5G Function Realization Program. Available online: https://b5g-rd.nict.go.jp/en/frp/ (accessed on 25 April 2024).
31. Eishima, T.; Inoue, S.; Yonemoto, A.; Sudo, J.; Hosonuma, T.; Nakasuka, S.; Shirane, A.; Tomura, T.; Okada, K.; Kiyohara, K. RF and Optical Hybrid LEO Communication System for Non-Terrestrial Network. In Proceedings of the IEEE International Conference on Space Optical Systems and Applications (ICSOS), Kyoto, Japan, 28–31 March 2022. [CrossRef]

32. Brashears, T. Achieving $\gtrless$99% link uptime on a fleet of 100G space laser inter-satellite links in LEO. In Proceedings of the SPIE Photonics West, San Francisco, CA, USA, 30–31 January 2024; Volume 12877. [CrossRef]

33. Darwish, T.; Kurt, G.K.; Yanikomeroglu, H.; Bellemare, M.; Lamontagne, G. LEO Satellites in 5G and Beyond Networks: A Review From a Standardization Perspective. *IEEE Access* **2022**, *10*, 35040–35060. [CrossRef]

34. Osoro, O.B.; Oughton, E.J. A Techno-Economic Framework for Satellite Networks Applied to Low Earth Orbit Constellations: Assessing Starlink, OneWeb and Kuiper. *IEEE Access* **2021**, *9*, 141611–141625. [CrossRef]

35. Al Homssi, B.; Dakic, K.; Wang, K.; Alpcan, T.; Allen, B.; Boyce, R.; Kandeepan, S.; Al-Hourani, A.; Saad, W. Artificial Intelligence Techniques for Next-Generation Massive Satellite Networks. *IEEE Commun. Mag.* **2024**, *62*, 66–72. [CrossRef]

36. Dakic, K.; Chan, C.C.; Al Homssi, B.; Sithamparanathan, K.; Al-Hourani, A. On Delay Performance in Mega Satellite Networks with Inter-Satellite Links. In Proceedings of the 2023 IEEE Global Communications Conference (GLOBECOM), Kuala Lumpur, Malaysia, 4–8 December 2023; pp. 4896–4901. [CrossRef]